

Savannah Journal of Science and Engineering Technology Volume: 01; Issue: 05; Pages: 291-299; 2023.

www.sajsetjournal.com.ng

DOI: xx.xxxx.x/sajset-01-2023-0059



Effect of silica and chemical modification on dispersion of carbon black nanoparticles in epoxy resin for use in smart materials

Joshua, R. M.

Mechanical Engineering Department, Modibbo Adama University, Yola, Adamawa State Nigeria.

Paper History

Received: 20th August, 2023 Accepted: 09th Sept, 2023 Published: Sept, 2023

Corresponding author: Joshua R. M. raphbari@yahoo.com

Abstract:

The addition of nanoparticles into organic polymers provides an efficient means to improve the properties of the matrix polymer. The properties of such polymer nanocomposites depend on the nanoparticles that are dispersed within the polymer matrix, as a result of incompatibility, the dispersion of synthesized inorganic nanoparticles in polymer matrices is very challenging, this paper report the synergistic effect of the use silica, thermal and chemical modification to improve the dispersion of carbon black (CB) nanoparticle in epoxy resin. The nanoparticles and the epoxy nanocomposite were investigated using XRD, XPS, FESEM, FTIR, BET/SAP, TEM and particle size zetasizer. The ESEM image shows a well dispersed CB nanoparticle within the host epoxy resin. The research considered the synergistic effects of silica addition, thermal treatment and chemical surface modification of Carbon black (CB) nanoparticle in the creation of a well dispersed network of conductive nanoparticle in epoxy. A nanocomposite coating over a laboratory modelled pipeline was generated; the nanocomposite was used as a piezoresistive sensor to capture vibration data as fluid is pumped through an experimental modelled pipeline.

Keywords: Carbon black, Dispersion, Epoxy resin, Nanoparticle, Nanocomposite, Silica

1. Introduction

There are several reasons for the development of nanopolymer compounds, such as improving physical, mechanical, and chemical properties, increasing lifespan, reducing costs, and decreasing negative environmental impact. The compatibility of polymer and nanofillers in the production nanocomposites is a challenge that needs to be studied, Polymer-based nanocomposites such as epoxy resin nanocomposites have become really vital engineering materials due to their exceptional properties and numerous application possibilities in modern technology [1].

In recent times, nanoparticles having outstanding physical and chemical properties have attracted deep interest and several methods have been developed to produce them. The addition of nanoparticles into organic polymers provides an efficient means to improve the properties of the host polymer such as electrical conductivity [2-6], mechanical properties [7, 8], thermal stability [9-11], flame retardancy, and resistance to chemical reagents. The properties of such polymer nanocomposites depend on the nanoparticles that are dispersed within the polymer matrix, including their surface chemistry, size, shape, concentration, and interactions with the polymer matrix [8]. However, the lack of compatibility between inorganic nanoparticles and polymer matrix restrict the applications of nanoparticles in polymer composites. As a result of incompatibility, the dispersion of synthesized inorganic nanoparticles in polymer matrices is very challenging, and nanoparticles characterized by high specific surface area and volume effects can easily form agglomerates. Hence, it is vital to modify the nanoparticles to reduce their tendency to agglomerate and improve their dispersion in polymer matrices.

Previously, numerous approaches consists of extensive mixing steps to achieve homogeneous distribution of fillers and to improve the polymer/filler interaction, however these approaches were of narrow achievement [12]. Hong and Chen [13] identified two ways that have been previously used to modify the surface of inorganic particles: modification of the surface by chemical treatment and the grafting of functional polymeric molecules to the hydroxyl groups existing on the particles. By surface modification of nanoparticles the dispersion of inorganic nanoparticles in organic solvents and polymer matrices is improved and Zhang et al. [14] reported the optimal dispersion of CB in epoxy resin in the presence silica network and recorded the creation of a conductive network between CB particles via direct particle contact and a tunnelling effect.

Epoxy resins are identified by their excellent chemical resistance, high specific strength, good dimensional firmness and adhesive properties. Epoxy resins can be used in liquids or powdered form, which ease their mixing with reactive or non-reactive modifiers. They are used as paints, coatings, adhesives and matrices for structural composites. However, once cured, epoxy resins

show a high crosslink density, which leads to bigger brittleness, low strain at break, reduced impact strength and little resistance to crack propagation [15]. Epoxy resins are thermoset polymer materials having two or more epoxide groups or oxirane rings in their molecular structure [16]. An epoxide is cyclic ether with a three-atom ring. While carbon black (CB) is an embodiment of basic carbon that is formed by guided vapor-phase pyrolysis and incomplete combustion of hydrocarbons [17]. The surface morphology of CB has a strong control on its wettability in polymer matrix and the properties of the ultimate polymer composites [18].

The morphology, physical and surface chemistry of CB can be improved chemically, thermally or photochemically in order to increase CB dispersion in a variety of media [12]. It has been proving that CB modified by coupling agent (Chemical Modification) shows a noticeable higher filler–polymer interaction which is obvious in the improvement of the mechanical properties and the enhancement of electrical conductivity of the composites [10].

Thermal treatment can stimulate oxidation of CB, thus increasing the amount of oxygen containing functional groups on the surface and even converting some proportion of the CB to CO or CO2 depending on the duration and temperature of the thermal treatment, thereby roughen the surface and increase the surface area [19]. However Kurt and Paul [20] states that when CB is heated in vacuum at a suitably elevated temperature, removal of the oxygen complexes occurs and the surface of the carbon particles is modified, they suggested a vacuum of 1 x 10-5 tor and a temperature of 1200 °C for 4 hours.

This study reports the synergistic effect of thermally treated of the CB nanoparticle in a controlled vacuum and

at a temperature of 600 °C and a vacuum of 1 x 10-5 torr (The vacuum is just enough to allow the removal of the natural oxidized group on the surface of CB), Chemical modification and the addition of silica nanoparticles. Electrically conductive polymer composites are favourable materials for numerous uses, such as rechargeable batteries, electromagnetic shielding, antistatic formulations, sensors, electronic devices, etc. Most electrically conductive polymer composites have been filled with conductive fillers, such as metallic particles or carbon black [21]. The major dynamics stirring up conductivity in nanocomposite is the percentage loading of the electrically conducting nanofiller, at low filler loading the conducting nanofiller are disjointed and electric current can flow only by way of tunnelling through a non-conducting medium between the neighbouring nanoparticles, the transport charge is not sufficient and conductivity is very low. As the nanofiller loading increases, resistance to charge transport get relaxed and conductivity steadily increases until percolation threshold is achieved where electrical conductivity sharply increases [22]. The conductivity of the epoxy carbon black nanocomposite changes under load as the newton value of the load changes, hence this property can be harness to sense variation in load such as vibration.

2. Smart Material: Mathematical Modelling

Epoxy resin/carbon black nanocomposite is known to display intergrain and grain boundary impedances and thus they can be represented by the equivalent circuit shown in Figure 1. The circuit consists of RC element connected in parallel, applying the Cole-Cole model we have the real and imaginary parts of the Cole-Cole impedance [23] as equation (1) and (2) respectively.

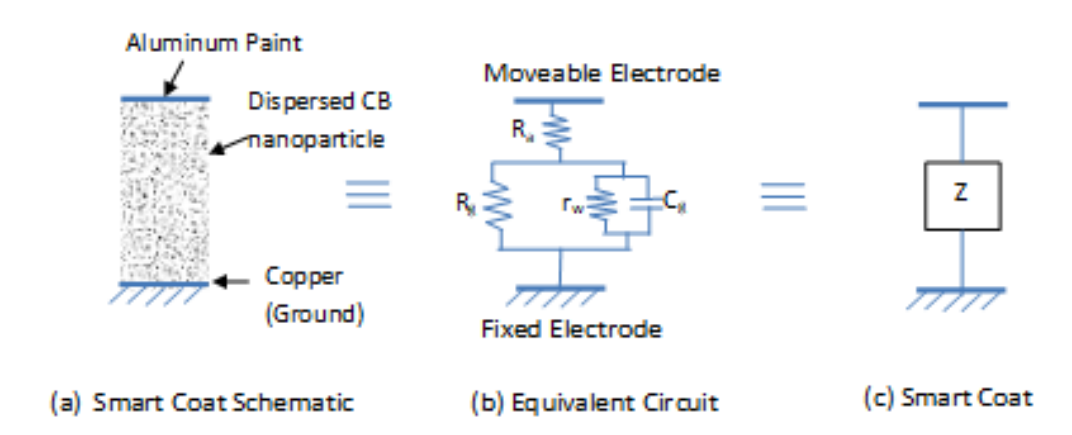


Figure 1: Equivalent Electric Circuit of the Nanocomposite Sensor

$$z' = R_a + \frac{R_e}{1 + (\omega \tau_{\omega})^2} \tag{1}$$

$$z'' = -\frac{\omega R_e \tau_\omega}{1 + (\omega \tau_\omega)^2} \tag{2}$$

Where R_a is the overall resistance of the CB nanoparticle aggregate, R_g is the resistance of the overall gaps of the nanocomposite, $\omega=2\pi f$, τ_{ω} is the frequency dependence characteristic time of the equivalent

circuit, Z is the impedance, \mathcal{C}_{ω} is the frequency dependence capacitance of the gap and

$$au_{\omega} = R_e C_{\omega} \text{ and } R_e = \frac{R_g \tau_{\omega}}{R_g + \tau_{\omega}}$$
 (3)

When the pipeline was excited by a force F(t) from the hammer, the mass m of the nanocomposite is displaced through a distance X(t). This mechanical disturbance is converted to an electrical signal.

When the disturbance is removed, the distance between the electrodes is x_0 and the distance becomes x_{dc} . When the voltage from the Hantek 365A USB multimeter data logger is applied. If K is the stiffness and b the damping coefficient of the nanocomposite then the stiffness force is given by equation 4 [24].

$$K_d = \frac{q_{dc}^2}{23A} \to x_{dc} = x_0 - \frac{q_{dc}^2}{23A}$$
 (4)

Where Q_{dc} is the charge in the electrodes due to dc bias \ni is the effective permittivity of the nanocomposite and A is the surface area of the electrodes. Applying the Hamilton principle for electromechanical systems and considering the Cole-Cole equations we have equation 5 [25]

$$\frac{d}{dt} \left(\frac{\partial L}{\partial \dot{z}_i} \right) + \frac{\partial D}{\partial \dot{z}_i} + \frac{\partial L}{\partial \dot{z}_i} = P_i \text{ and}$$

$$\frac{d}{dt} \left(\frac{\partial L}{\partial \dot{Q}_k} \right) + \frac{\partial D}{\partial \dot{Q}_k} + \frac{\partial L}{\partial \dot{Q}_k} = E_k$$
(5)

Where P_i includes all non-consecutive mechanical loads which are not included in the dissipation function and E_k is the non-consecutive voltage [25]. The dissipation energy function D is given by equation 6 [25].

$$D = \frac{1}{2} \left(b \dot{x}^2 + (R_0 + R_a) \bar{Q}_1^2 + R_g (\bar{Q}_1 - \bar{Q}_2)^2 \right) \quad (6)$$

and the virtual work [25] is shown in equation 7

$$\delta W_{nc} = F(t)\delta x + u_{in}\delta \bar{Q}_i \text{ or}$$

$$\delta W_{nc} = \sum_{i=1}^n P_i \delta \dot{z}_i + \sum_{i=1}^l E_k \delta \dot{Q}_i$$
 (7)

The electrical charge in the nanocomposite is given by equation 8 [25]

$$\dot{Q}_1(t) = Q_{1dc} + Q_1$$
 and $\dot{Q}_2(t) = Q_{2dc} + Q_2$ (8)

Where Q_{idc} (i = 1, 2) is the charge due to a DC bias and $Q_i(t)$ is the charge created by the excitation. The Lagrangian is given by equation (9).

$$L = T'' - V - W_e \tag{9}$$

Where T" is kinetic energy given by $\frac{1}{2}m\dot{x}^2$, V is the potential energy given by $\frac{1}{2}(x+d)^2$, and W_e is the internal electrical energy given by $\frac{1}{2C_q}\bar{Q}_2^2$

Substituting equations 6 to 8 into equation 5, we have

$$m\ddot{x} + b\dot{x} + Kx - \frac{Q_{2dc}}{2A}Q_2 = F \tag{10}$$

$$(R_0 + R_a)\dot{Q}_1 - R_g(\dot{Q}_2 - \dot{Q}_1) = 0$$

$$R_g(\dot{Q}_2 - \dot{Q}_1) + \frac{x_{dc}}{\ni A}Q_2 - \frac{Q_{2dc}}{\ni A}x = 0$$
(11)

Equations (10) and (11) are the model equations of the nanocomposites

3. Methodology

3.1 Materials

The CB used is commercially available Vulcan® XC72R manufactured by Cabot Corporation. The CB is a

specialty type use for power storage, including batteries and fuel cells, Conductive paper, Conductive liquid dispersions and Catalyst support. The specification of Vulcan® XC72R is shown in Table 1 below

Table 1: Properties of Carbon Black

Sample	Property	Value	Unit
XC72R	OAN	192	cc/100g
XC72R	Tint	87	%
XC72R	Mesh Residue	<10	ppm
XC72R	Iodine Number	253	Mg/g
XC72R	Specific gravity	1.7	g/cm3
XC72R	Bulk Density	200-680	Kg/m3

The silica (SiO₂) nanoparticle with 10-25 nm diameter was obtained from Zhengzhou Dongshen Petro Chemical Technology Co, Ltd. 3-Aminopropyltrimethoxysilane (APTMS) was manufactured by Sigma Aldrich with a refractive index of 1.424, boiling point of 91-92 °C and density of 1.027 g/ml at 25 °C.

3.2 Experiment

100 g of CB was measured into a crucible and put into Berkeley inert gas vacuum heat treatment furnace shown in Figure 2. The CB sample is heated to 600 $^{\circ}$ C in 1 hour at a heating rate of 10 $^{\circ}$ C/min and a vacuum pressure of 200 mbar. The sample was retained at 600 $^{\circ}$ C for ½ hour and then cooled to 25 $^{\circ}$ C in 3 hours the sample was then removed and the mass loss was measured using a weigh balance.

3.3 Surface Modification of CB

To modify the surface of the thermally treated CB at 600 °C (CB600), APTMS and Acetone solution was prepared by diluting with distilled water to obtain a well dispersed balanced solution. The CB600 was poured into the solution and mixed by stirring manually prior to sonication for 30 minutes. The solution was further stirred using a magnetic stirrer at a temperature of 60 °C for 30 minutes. The entire content was then filtered to obtain the surface treated CB nanoparticles. The wet nanoparticles were dried in an oven at 100 °C for 24 hours.

3.4 Dispersion of CB in Epoxy Resin

170g of epoxy was poured into beaker (A) and preheated for 30 minutes at 40 °C to improve viscosity. 20 % nano silica with respect to CB %wt. was measured and added to the beaker containing 170g of epoxy. The mixture was stirred manually until a homogenous mixture was achieved. 12.5 %wt. of CB with respect to epoxy resin content was placed into another beaker (B) containing 250 ml of acetone, 4.6 % of APTMS with respect to %wt. of CB was also added. The content of the beaker (B) is manually mixed before the sonication process. Sonication was done with an ultrasonic cleaner model 008 with an ultrasonic power of 50 w and a frequency of 40 kHz. The sonication process proceeded for 15 minutes at a time and a break period of 2 minutes

between intervals. After 60 minutes of sonication, the content of the beaker containing acetone was poured into the beaker (A) containing epoxy resin, the content is stirred manually until a homogenous mixture. The beaker was then placed on a magnetic stirrer, the temperature was set to 60 °C and the speed was adjusted to 950 rpm. The magnetic stirring was done a duration of 60 minutes while maintaining the temperature at 60 °C to ensure proper dispersion. Further stirring was done using a mechanical mixer at 600 rpm for 30 minutes; the mechanical mixer used was a pensonic PM-112 hand mixer with an electrical power of 120 w and a 5-speed selection. The sample was then placed in the degassing chamber and the vacuum pump was operated for 30 minutes to remove air bubbles trapped within the sample.

The resin-hardener ratio of 100:29 as advised by the manufacturer was adopted; 49.3g of curing agent was added to the degassed sample and mixed manually until a homogenous mixture was achieved. The nanocomposite was then poured into the molds shown in Figures 3.4-3.8 and allowed to cure at room temperature for 24 hours. The mold for the sample contains 4 cavities with dimension 50 x 50 x 5 mm each for the production of the test sample. The samples were post cured for 60 minutes at 100 $^{\circ}$ C in an oven to complete the curing action. This procedure was repeated to produce three other sample; CB without silica, CB600 without silica and CB600 modified with APTMS but without silica.

3.5 Characterisation

CB and the SiO₂ nanoparticle were characterize using X-ray photo spectroscopy (XPS) to obtain the surface chemistry, the chemical state of the samples at the surface to a maximum depth of 10 nm was studied by irradiating the sample with a beam of x-ray in an ultra-high vacuum of pressure less than 10-9 mbar. The kinetic energy is then measured and the number of electrons that escape the surface was counted to identify the elemental composition, the empirical formula, electronic and chemical state of the sample at the surface. Using vacuum transfer module for moving airsensitive samples the nanomaterial samples were transferred from a glove box into the K-alpha XPS made by Thermo Scientific shown in Figure 3.16. The samples were subjected to several cycles of XPS analysis and ion beam sputtering to assemble the final XPS depth outline. High resolution XPS spectrum were collected with integrated monochromatic dual mode ion source (1486.68 eV) in inspection manner with a small spot size of 400 µm, pass energy of 200 eV for the survey scans. and 70 eV for the elemental scans. Spectrum was then obtained at each emission angles by tilting the specimens. Data analysis was performed with Avantage[©] software (Thermo Scientific). Normally, 10 scan integration were enough for acquiring elemental spectra with high signal to noise ratio.

The nanocomposite, as received and the modified nanoparticles were characterized to determine their diffractogram showing amorphous and crystalline

phases, phase concentration (area covered by the peaks) and crystalline size. The epoxy resin-CB-SiO $_2$ nanocomposite was grinded with hack saw blade before the XRD analysis, the XRD analysis was done using X'Pert $_3$ Powder PANalytical. Powdered sample was scanned from 2-79.99 $^{\rm o}$ in 2 theta scope with 0.026261 $^{\rm o}$ movement interval and 2s per step response time. The anode material of the X'Pert $_3$ Powder PANalytical is copper (Cu) with K-Alpha1 wavelength of 1.540598 A $^{\rm o}$ and K-Alpha2 wavelength of 1.544426 A $^{\rm o}$. Origin lab 8.0 software was used for deconvolution of the diffractogram in the 2-theta region of 18-32 $^{\rm o}$.

To obtain surface area, the nanoparticles were dried at 100 °C in an oven for 12 hours. The experiment was conducted using Micromeritics Tristar II surface area and porosity analyzer, 0.1948 g of the sample was measured, the experiment was conducted with a warm free space of 15.5504 cm³ and a cold free space of 47.0609 cm³. The analysis bath temperature was kept at -195.800 °C during the experiment with an accompanied automatic degassing process. Figure 3.18 showed the Micromertics Tristar II surface area and porosity, the porosity distribution was calculated using the Barret-Joyner-Hallender (BJH) method and the surface area was calculated using the Brunauer–Emmett–Teller (BET) method.

The FTIR analysis was carried out using the Pelkin Elmer-Spectrum One FTIR spectrometer. The samples were run from 4000 cm⁻¹ to 450 cm⁻¹ with eight scans at a scan speed of 0.20 cm/s and a resolution of 4.00 cm⁻¹. For the nanocomposite the samples were cut into smaller pieces to produce a fresh surface for analysis. Each sample was placed on the ATR diamond so that it was entirely covered and the sample was analysed. The resulting spectrums were normalized to 1.0 and their major peaks were labelled to show the various groups accordingly.

The elemental constituent, particle size and surface morphology of the nanoparticles and the produced nanocomposite were investigated using a Zeiss Supra55 VP variable pressure FESEM equipped with energy dispersive x-ray (EDX) microanalysis system. The system distinguishes the x-rays emitted from the test pieces because of the rich-energy electron ray penetrating into the sample. The x-ray spectra were retrieved and examined, to obtain a quantitative data of the basic constituent of the test piece. The procedure has an accuracy of 1-2 % for a number of elements down to 0.1 weight percent. Prior to the analysis the samples were gold spayed to ensure accurate imaging and the penetration and reflection of the x-rays

A Zeiss Libra 200 model TEM was used for the morphological studies of the nanoparticles samples, the sample was dispersed in methanol solvent using sonication for 30 minutes. Drops of the suspension were placed on lacey carbon grids for electron microscopy analysis. The sample was dropped into the sample holder of Zeiss Libra 200/FEG TEM working at 200 kV with Koehler illumination. The area having the sample was found in TEM mode and using a condenser aperture

of 15 μ m and a convergent beam size of 5 nm, the large angle dark-field STEM imaging utility of the Libra was used to acquire a scanning image of the located area. To acquire a clear diffraction pattern, the STEM stationary beam utility of the Libra was then use to create a small, nearly parallel beam with a diameter of 300 nm. Figure 3.21 shows the Zeiss Libra 200 model.

The particle size distribution and the zeta potential of the nanoparticle in acetone were studied using the Malvern zetasizer Nano ZSP. 1g of nanoparticle was dispersed in 100 cm³ of acetone using ultrasonic bath, the solution was sonicated for 1 hour with 2 minutes rest period after

every 15 minutes of sonication. 1 cm³ of the nanoparticle dispersed solution was poured into the glass cuvette and placed into the zetasizer. The Zetasizer uses dynamic light scattering (DLS) or photon correlation spectroscopy to measure the particle size in the order of sub-micron. DLS measures the Brownian motion of the nanoparticle in solution and relates it to the size of the nanoparticles.

4. Result and discussion

The results for the experiments were shown in the following Figure 2 to 9.

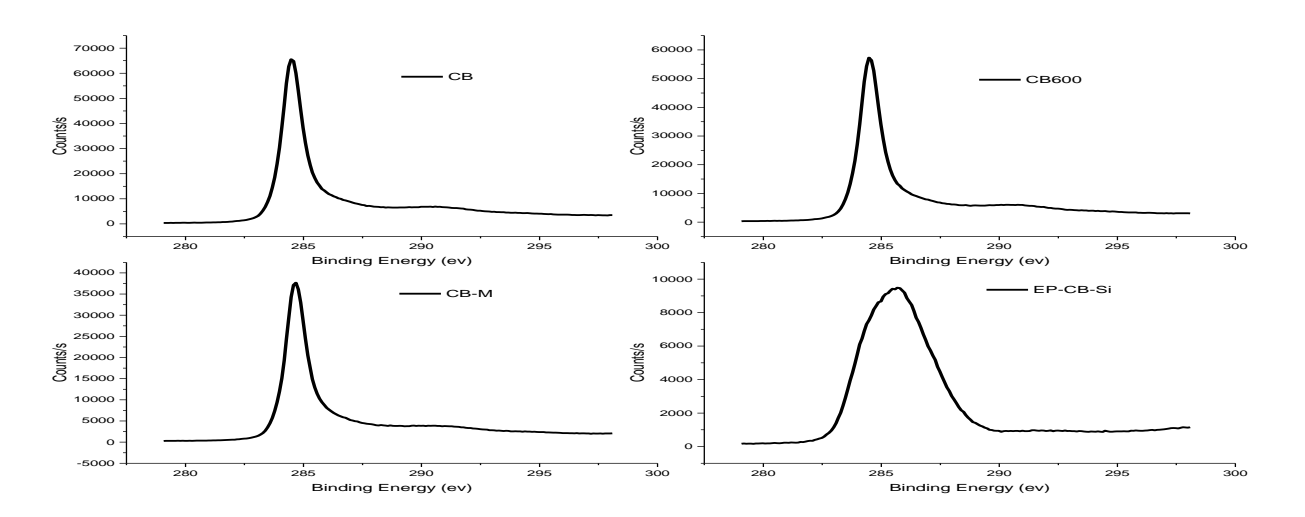


Figure 2: C1s Scan of the nanocomposite Carbon Black Nanoparticle

XPS is a powerful analytical technique to evaluate compositions of CB nanoparticle by establishing data about the surface chemistry (up to a sample depth of about 10 nm). The XPS analysis as shown in Figure 1

consists of a C1s peak at 284.58 and 532.98 eV respectively. For the CB nanoparticle the graphitic character influences the surface free energy as indicated by C1s peak at 284.58 eV.

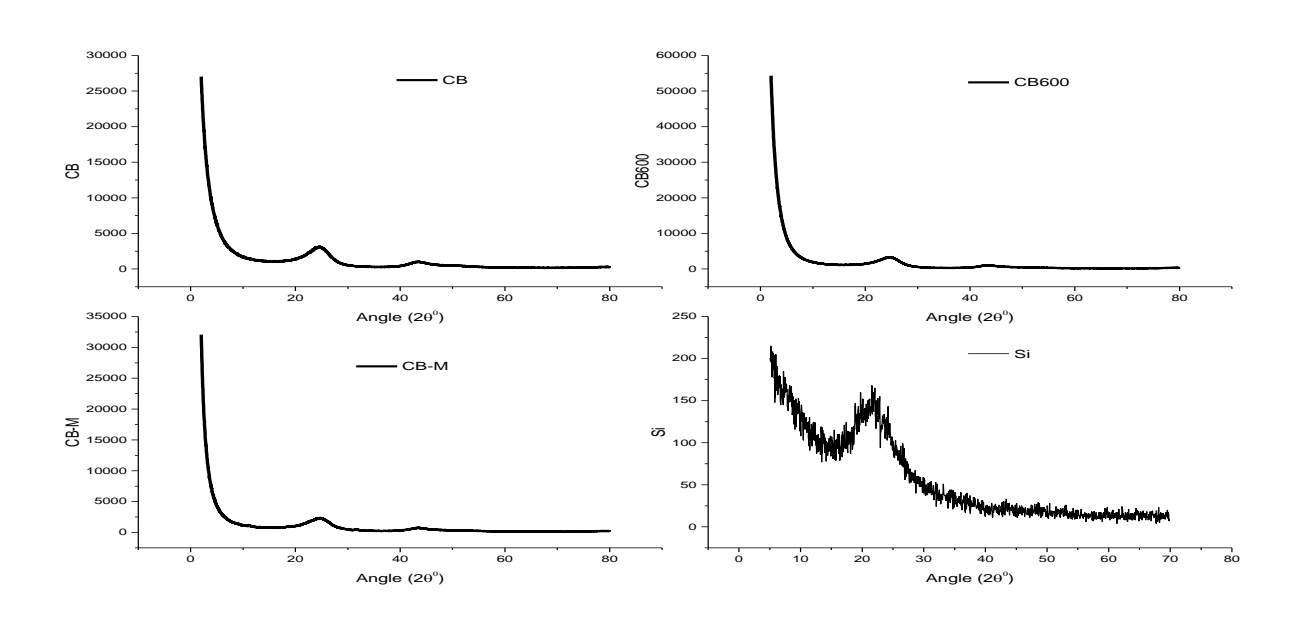


Figure 3: XRD of Silica and Carbon Black Nanoparticles

The XRD profiles of the samples are presented in Figure 3 There are unique peaks at 22.410 of high intense for the CB and a little broadening with the thermally treated CB. The broadening is a result of formation of high structure and tendency to form an amorphous structure. It has been shown by previous research that the electrical conductivity of carbonized fiber increases with the increase in heat treatment temperature [26], this can

be confirm due to the existence of an increasing high structure. CB nanoparticle is known for its high surface area however as shown in Figure 4 vacuum thermal treatment did increase the surface of the CB. The surface area of the CB nanoparticle increases with increase in the heat treatment temperature. The increase in the surface area of the CB nanoparticle could be attributed to increase in burn off.

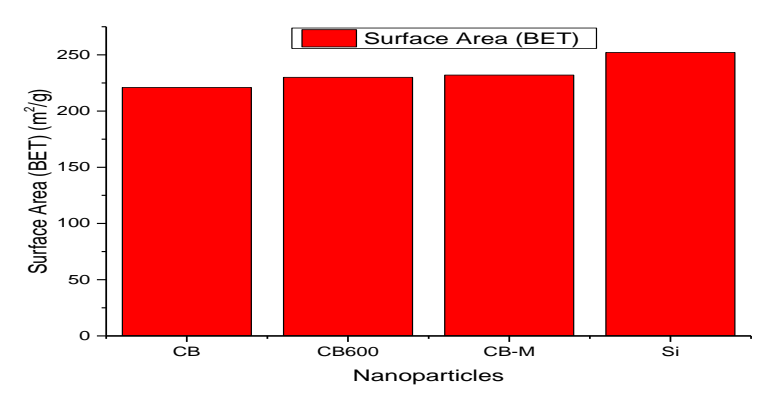


Figure 4: Surface area of Nanoparticle

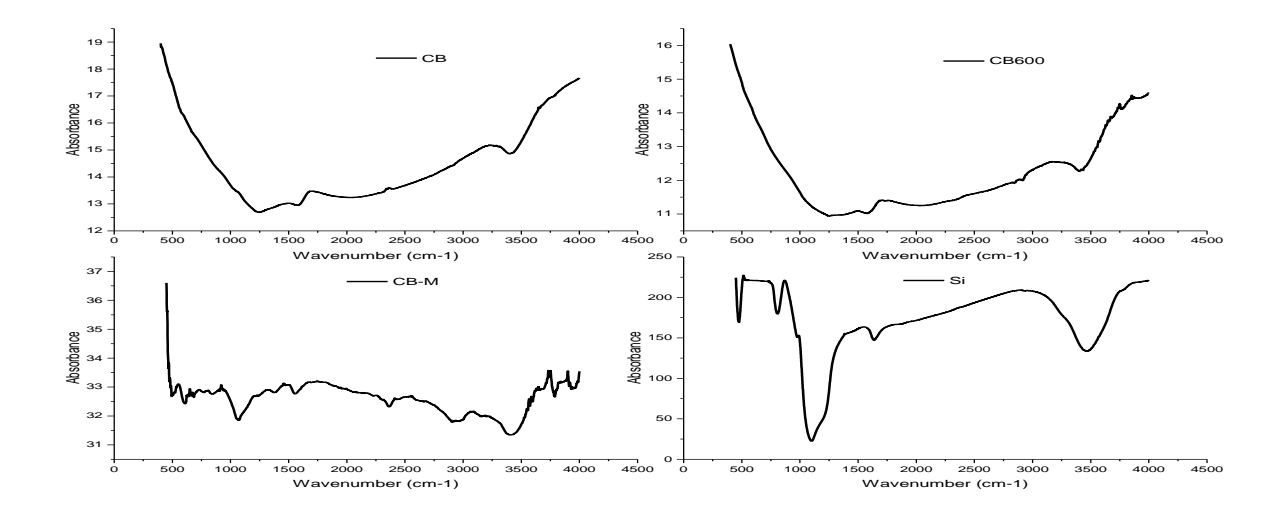


Figure 5: FTIR of Nanoparticle

Figure 5 shows the FTIR spectrum of CB samples, regarding the thermally oxidized sample at 600 0C a visible but broad peak is shown near the 3200 -3700 cm-1 indicating the presence of hydroxyl group with the Chemical modified carbon black showing the existence of additional functional group with a broad peak of 3929 cm-1, therefore a more hydroxyl enrich surface is obtained.

Figure 6a and 6b shows FESEM images of the asreceived CB and thermal treated CB nanoparticle sample respectively. The morphologies across the two (2) nanoparticle samples indicate that nanoparticles are agglomerated and are within 20.59–69.90 nm particle size.

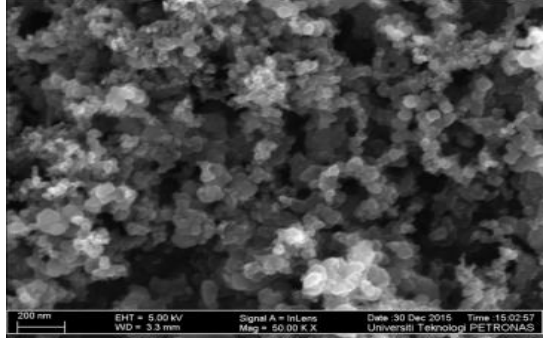


Figure 6a: FESEM Image of (a) as Received CB

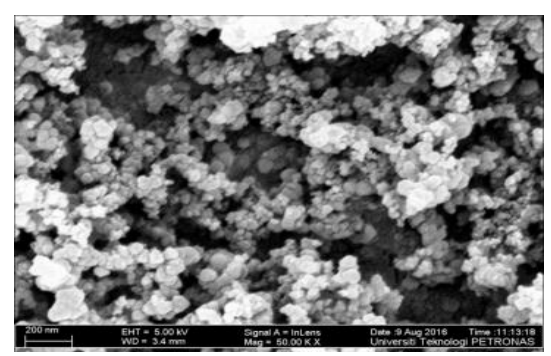


Figure 6b: FESEM Image of Thermal treated CB and

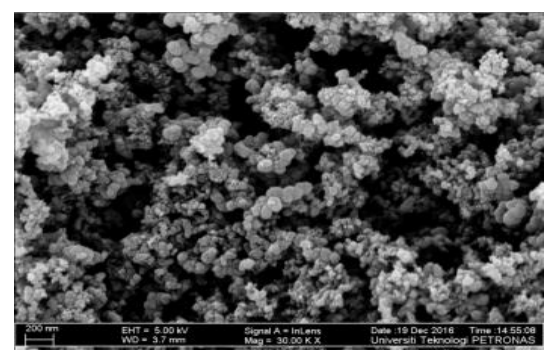


Figure 6c: FESEM image of thermally and chemically modified CB (50 K magnification)

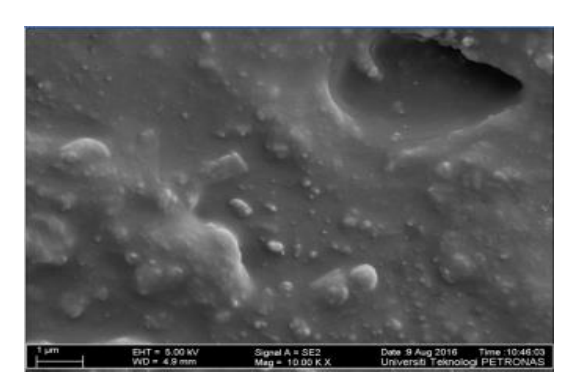


Fig. 7a: FESEM Image of Epoxy Nanocomposite Received CB

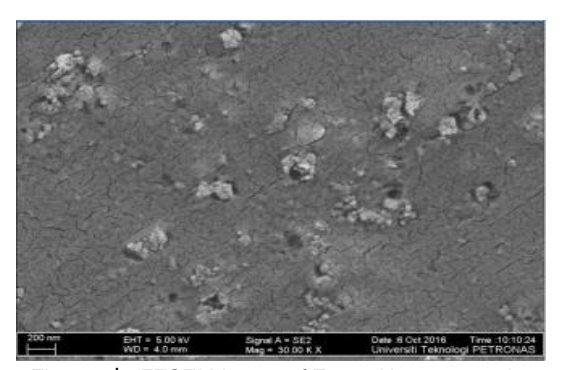


Figure 7b: FESEM Image of Epoxy Nanocomposite
Thermal treated CB

Furthermore, CB primary particles are spherical and merged together forming aggregates due to Van der *Waals* forces. The structure of carbon black particles ranges from crystalline to amorphous materials. Figure 6c shows a less agglomerated CB nanoparticle as result

of both thermal and chemical modification of the nanoparticle.

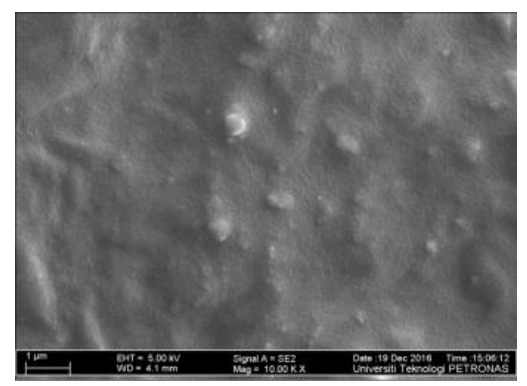


Figure 7c: FESEM Image of Epoxy Nanocomposite Thermally and chemically modified CB

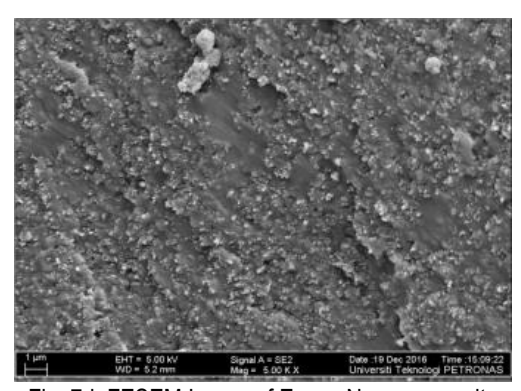


Fig. 7d: FESEM Image of Epoxy Nanocomposite
Thermally and chemically modified CB in the presence of
Silica (30 K magnification)

Figure 7a shows a nanocomposite of epoxy and highly agglomerated as received CB, in Figure 7b the nanocomposite form site of distantly distributed agglomeration of the thermally treated CB/ In contrast Figure 7c shows a fairly dispersed CB nanoparticle within the epoxy matrix due synergistic effect of Thermal and chemical modification Figure 7d shows the epoxy resin nanocomposite with a well dispersed network of CB nanoparticle in the presence of silica nanoparticles. The particle size distribution as shown in Figure 8 indicates a shift to the left as the heat treatment temperature increases. It is obvious that vacuum thermal treatment improves the particle size distribution of CB in acetone.

4.1 Vibration measurement using the Nanocomposite

The sample of the epoxy nanocomposite produced was used as paint to generate coating of 1 mm thickness over a pipeline of external diameter of 30 mm and length of 2830 mm containing flowing water. Aluminum paint was then applied over the nanocomposite coating to act as an electrode. A Handtek multimeter was used to capture the variation in the resistance of the conducting epoxy nanocomposite as the water flows which represent the vibration of the pipeline caused by the flowing water as shown in Figure 9.

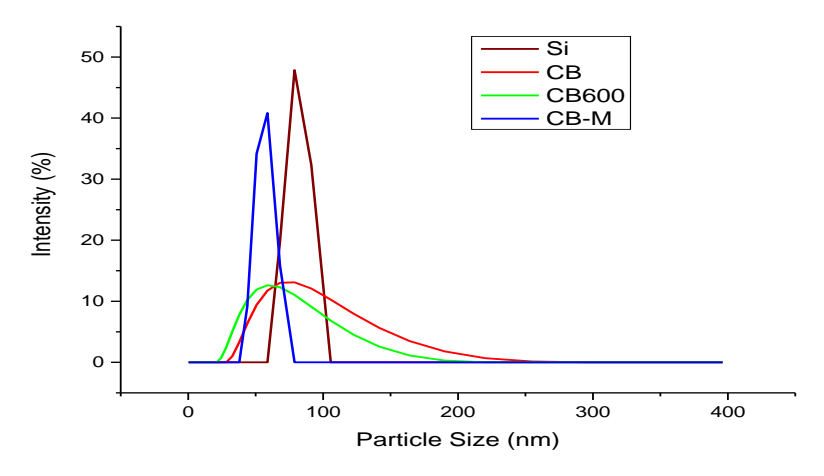


Figure 8: Particle size distribution of the nanoparticles in acetone

Variation in frequency and amplitude for the vibrating pipeline with time is captured by the EMD energy spectrum as shown in Figure 9. The energy spectrum for the pipeline is marked by lower frequency peak over a longer period occurring after 500s as shown in Figure 9.

The result obtained shows that the generated epoxy nanocomposite paint is a smart material that can be used in structure to monitor the health of the structure when subjected to loading.

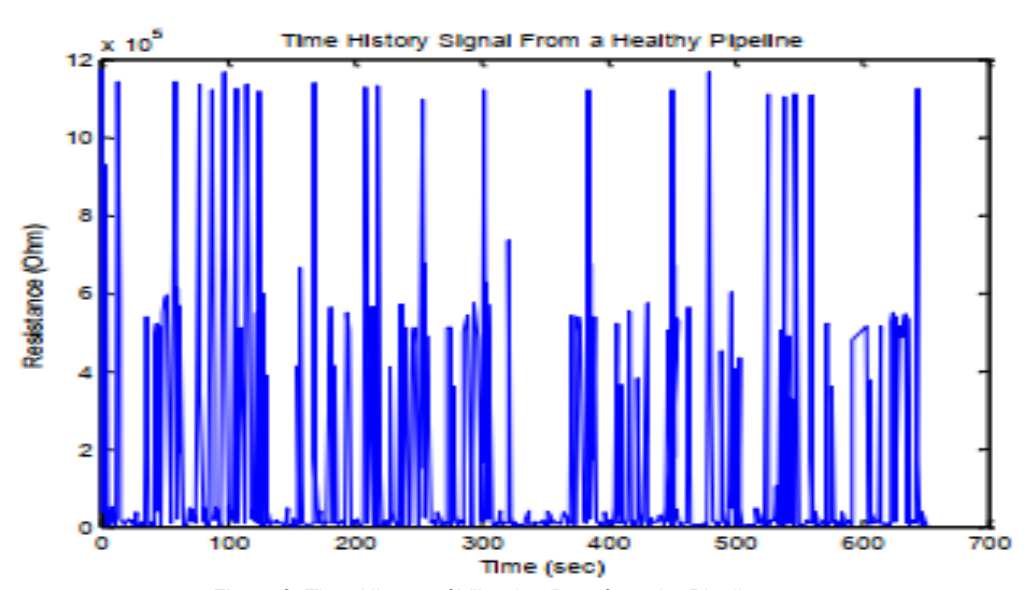


Figure 9: Time History of Vibration Data from the Pipeline

5. Conclusions

Thermal treatment of the CB Nanoparticles resulted in burn off with consequent increase in surface area of the nanoparticles and an increase in the hydroxyl functional group. The chemical treatment of the CB stimulated the oxidation of the surface of the nanoparticle as shown by the functional groups in the FTIR spectrum of Fig. 3. The thermal treatment provided a roughen surface for better silanization of the nanoparticle during the chemical treatment. The addition of silica nanoparticles in the epoxy resin lowered shrinkage on curing, decrease thermal expansion coefficients and improve adhesion properties while creating the disperse network of CB within the epoxy. The modification done assisted in the production of a

smart epoxy material for the capturing of vibration data over a pipeline

References

- [1] Damircheli, M. and MajidiRad, A., (2023). The Influence of the Dispersion Method on the Morphological, Curing, and Mechanical Properties of NR/SBR Reinforced with Nano-Calcium Carbonate, *Polymers (Basel)*, 15, 1-13
- [2] Yuan, Q. and Wu, D. Y., (2010). Low Percolation Threshold and High Conductivity in Carbon Black Filled Polyethylene and Polypropylene Composites, *Journal of Applied Polymer Science*, 115, 3527–3534.

- [3] Krupa, I., Cecen, V., Boudennec, A., Prokeš, J. and Nováke, I., (2013). The Mechanical and Adhesive Properties of Electrically and Thermally Conductive Polymeric Composites Based on High Density Polyethylene Filled with Nickel Powder, *Material Design*, 51, 620–628.
- [4] Bhuiyan, M. K. H., Rahman, M. M., Minab, M. F., Gafur, M. A. and Begum, A., (2013). Crystalline morphology and properties of multi-walled carbon nanotube filled isotactic polypropylene nanocomposites: Influence of filler size and loading, *Composites*, Part A, 70–79.
- [5] Ameli, A., Jung, P. U. and Park, C. B., (2013). Electrical Properties and Electromagnetic Interference Shielding Effectiveness of Polypropylene/Carbon fiber Composite Foams, *Carbon*, 60, 379-394.
- [6] Cagliostro, D. E., (1980). Carbon Fiber Production at Low Temperatures from Polyacryonitrile, *Textile Research Journal*, 50, 632-638.
- [7] Bin, Y., Yamanaka, A., Chen, Q., Xi, Y., Jiang X. and Matsuo, M., (2007). Morphological, Electrical and Mechanical Properties of Ultrahigh Molecular Weight Polyethylene and Multi-wall Carbon Nanotube Composites Prepared in Decalin and Paraffin, *Polymer Journal*, 39, 598-609.
- [8] Marra, F., D'Aloia, A. G., Tamburrano, A., Ochando, I. M., Bellis, G. D. and Ellis, G., (2016). Electromagnetic and Dynamic Mechanical Properties of Epoxy and Vinylester-Based Composites Filled with Graphene Nanoplatelets," Polymers, 8, 1-18.
- [9] GÜLtekİN, N. D., (2015). Investigation of Thermal and Electrical Conductivity Properties of Carbon Black Coated Cotton Fabrics, Marmara University Journal of Science, 27, 1-15.
- [10] Ding, X., Wang, J., Zhang, S., Wang, J. and Li, S., (2015). Carbon black-filled polypropylene as a positive temperature coefficient material: effect of filler treatment and heat treatment, *Polymer Bulletin*, 73, 369-383.
- [11] Pahalagedara, L. R., Induni, W., Siriwardane, N. D., Tissera, R. N., Wijesena, K. and de Silva, M. N., (2017). Carbon black functionalized stretchable conductive fabrics for wearable heating applications, *RSC Advances*, 7, 19174-19180.
- [12] Atif, M., (2014). Surface modification and characterization of carbon black; UV cured colored epoxy composites, PhD Dissertation, Materal Science, DISAT, Politecnico di Torino, Italy.
- [13] Hong R. Y. and Chen, Q. (2015). Dispersion of Inorganic Nanoparticles in Polymer Matrices: Challenges and Solutions, in *Organic-Inorganic Hybrid Nanomaterials*, 267, in Kalia, S. and Haldora, Y. Eds., ed Switzerland: Springer International Publishing, pp.1-38.

- [14] Zhang, W., Blackburn, R. S. and Dehghani-Sanij, A. A. (2007). Effect of Silica on the Electrical Properties of Epoxy of Phenolic Resin/Carbon Black/Silica Composite Coating, Scripta Materialia. 56, 581–584.
- [15] Bialkowska, A., Bakar, M., Kucharczyk, W. and Zarzyka, I., (2023). Hybrid Epoxy Nanocomposites: Improvement in Mechanical Properties and Toughening Mechanisms-A Review, *Polymers (Basel)*, 15, 1-13
- [16] Bauer, R. S., (1983). Epoxy Resin Chemistry II vol. 221. Washington D.C.: American Chemical Society.
- [17] Long, C. M., Nascarella, M. A. and Valberg, P. A., (2013). Carbon black vs. black carbon and other airborne materials containing elemental carbon: Physical and chemical distinctions, *Environmental Pollution*, 181, 271-286.
- [18] Martinez, L., Nevshupab, R., Felhcs, D., de Segovia, J. L. and Roman, E., (2011). Influence of Friction on the Surface Characteristics of EPDM Elastomers with Different Carbon Black Contents, *Tribology International*, 44, 996–1003.
- [19] Frysz, C. A. and Chung, D. D. L., (1997). Improving the electrochemical behavior of carbon black and carbon filaments by oxidation, *Carbon*, 35, 1111-1127.
- [20] Kurt, S. D. and Paul, E. T., (1992). The Effect of Thermal Processing in Vacuum on the Water Adsorption Characteristics of Carbon Black, Material Research Society Symposium Proceeding, 270, 67-72.
- [21] Jia, Q. M., Li, J. B., Wang, L. F., Zhu, J. W. and Zheng, M., (2007). Electrically conductive epoxy resin composites containing polyaniline with different morphologies, *Materials Science and Engineering*, A, 448, 356-360.
- [22] Blythe, T. and Bloor, D., (2005). *Electrical Properties of Polymer*. New York: Cambridge University Press.
- [23] Ahmadu, U., Tomas, S., Jonah, S. A., Musa, A. O. and Rabiu, N., (2013). Equivalent circuit models and analysis of impedance spectra of solid electrolyte Na0.25Li0.75Zr2(PO4)3, Advanced Material Letters, 4, 185-195.
- [24] Aldraihem, O. J., Akl, W. N. and Baz, A. M., (2009). Nanocomposite Functional Paint Sensor for Vibration and Noise Monitoring, Sensors and Actuators, A, 233–240.
- [25] Preumont, A. (2006). *Mechatronics Dynamics of Electromechanical and Piezoelectric Systems*. Dordrecht, Nertherland, Springer.
- [26] Geiderik, M. A., Davydov, B. E., Krentsel, B. A., Kustanovich, I. M., Polak, L. S. and Topciev, A. V., (1961). Preparation of Polymeric Materials with Semiconductor Properties, *JournalL of Polymer Science*, 54, 621-626.